Option-Implied Preference with Model Uncertainty

Byung Jin Kang[1], Tong Suk Kim[2], Hyo Seob Lee[3]

Preliminary draft: 2013

Abstract

We present a theoretical model of option-implied preferences with model uncertainty. An option-implied risk aversion function with model uncertainty has a higher and a steeper level of risk aversion than an investor without model uncertainty. Based on the theoretical model, we try to extract empirical option-implied risk aversion functions with S&P 500 index options. Our empirical option-implied risk aversion and option-implied uncertainty premium show decreasing and smirk pattern across wealth, which helps to explain the smirk pattern of implied volatility as well as the negative volatility spread.

JEL classification: G13; C13;

Keywords: model uncertainty; option-implied risk aversion; volatility smirk

[1] Soongsil University School of Finance, 511 Sangdo-Dong, Dongjak-Gu, Seoul, 156-743, Republic of Korea, bjkang@ssu.ac.kr

[2] Graduate School of Finance, KAIST, 87 Hoegiro, Dongdaemoon-gu, Seoul, 130-722, Republic of Korea, tskim@business.kaist.ac.kr

[3] Corresponding author, Korea Capital Market Institute, 45-2 Youido-dong, Youngdungpo-gu, Seoul, 150-974, Republic of Korea, hslee@kcmi.re.kr

1. Introduction

Asset prices reflect investors' risk preferences. Especially option prices with leveraged and different strike prices contain important risk preferences such as risk aversion, uncertainty aversion. Previous literatures mainly dealt with option-implied risk aversion, not with an aversive attitude of uncertainty. Jackwerth (2000) and Aït-Sahalia (2000) derive option-implied risk aversion functions. Bliss and Panigirtzoglou (2004) and Kang and Kim (2006) also estimate option-implied risk aversion functions with the time varying property of subjective density. Rosenberg and Engle (2002) suggest a counter cyclical risk aversion from S&P 500 option prices. Bakshi and Madan (2006) shows that the disparity between implied volatility and realized volatility is affected by an investors' risk aversion. Unlike those literatures, we focus on the option-implied uncertainty preference disentangled from option-implied risk aversion.

An uncertainty aversion is differentiated from a risk aversion. A risk aversion measures an aversive attitude from known distribution, but uncertainty aversion reflects an aversive attitude from unknown distribution. Knight (1921) first mentioned the difference between risk and uncertainty, and Ellsberg (1961) introduces a paradox that an investor with unknown distribution prefers the choice of violating the expected utility hypothesis. Gilboa and Schmeidler (1989), Chen and Epstein (2002), Epstein and Wang (1994) incorporate a Knightian uncertainty in the economic model. Anderson, Hansen, and Sargent (2003), Hansen and Sargent (2001, 2008), Maenhout (2004, 2006) develop a robust control theory along the line of an uncertainty framework. These studies usually deal with a stock price, and a few studies mentioned derivatives assets such as futures and options. Lien and Wang (2003) examines the effect of Knightian uncertainty in the commodity futures market, and Liu, Pan, and Wang (2005) explains the volatility smirk pattern with model uncertainty. This paper attempts to examine the effect of a model uncertainty in the equity options market.

As the first contribution, we present a theoretical framework of option-implied risk aversion with a model uncertainty. We set up an equilibrium model for a robust agent who has both a reference model and an alternative worse-case model, and the robust agent worries about a pessimistic scenario. She wants to maximize her terminal wealth and simultaneously minimizes the difference between the reference model and the alternative model. By solving this min-max utility problem, we derive the option-implied risk aversion function with model uncertainty, which produces higher level of risk aversion than the traditional option-implied risk aversion without model uncertainty.

The second contribution is that we empirically derive both the option-implied risk aversion functions with model uncertainty and the related option-implied uncertainty premium by using S&P 500 index options. It had been generally known that option-implied risk aversion functions show a decreasing or U-shaped[4]. In addition, the implied volatility of equity option had been known with a smirk pattern as stated in Rubinstein (1994). Our empirical option-implied risk aversion with model uncertainty shows decreasing and smirk pattern, which helps to explain this decreasing property of option-implied risk preferences and related volatility smirk pattern especially in negative wealth regions. Furthermore, the empirical option-implied uncertainty premium in addition to the equity premium could give a tip of negative volatility risk premium in Bakshi and Kapadia (2003).

The remainder of this study is organized as follows. In section 2, we construct an equilibrium model for deriving an option-implied risk aversion with model uncertainty. In Section 3, by using Option Metrics Ivy Database, we empirically estimate the option-implied risk aversion functions with model uncertainty and offer the option-implied uncertainty premium. Finally, in Section 4, we give a conclusion.

[4] Ziegler (2007) tries to explain why the option-implied risk aversion functions can be a smile. Theoretically He gives three reasons of this smile pattern: (i) preference aggregation with and without stochastic volatility and jumps; (ii) mis-estimation of investor beliefs due to stochastic volatility and jumps, or Peso Problem; (iii) heterogeneous beliefs.

2. Model

2.1 Problem without model uncertainty

We consider a continuous time financial market that has one riskless asset and one risky asset in the finite time horizon [0, T]. A riskless asset follows the deterministic process with the drift r, where is risk-free rate. A risky asset follows a stochastic differential equation where μ and σ are the drift and volatility, where B_t is a standard Brownian motion on a probability space $\{\Omega, F, P\}$, and $\{F_t: t\in[0,T]\}$ is a filtration generated by the Brownian motion.

$$dS_t = \mu S_t dt + \sigma S_t dB_t \tag{1}$$

Let us define the market price of risk, and the state-price density or stochastic discount factor, respectively as follows.

$$\theta = \frac{\mu - r}{\sigma}, \quad H_t = \exp\left\{-\theta B_t - \left(r + \frac{1}{2}\theta^2\right)t\right\} \tag{2}$$

Without an intermediate consumption, the representative agent chooses an optimal dollar amount of stock investment, π_t. The wealth process W_t evolves according to the following stochastic differential equation, which implies the investor's budget constraint.

$$dW_t = \left\{rW_t + (\mu - r)\pi_t\right\}dt + \pi_t \sigma dB_t, \quad W(0) = w \tag{3}$$

We do not assume that the agent has a specific utility. Controlling the stock investment π_t, the agent faces the following terminal wealth maximization problem.

Problem 2.1 *The agent maximizes her utility with a budget constraint*

$$
\begin{aligned}
&V(w) = \sup_{\pi_t} E\left[u(W_T)\right] \\
&s.t \\
&dW_t = \left\{rW_t + (\mu - r)\pi_t\right\}dt + \pi_t \sigma dB_t, \quad W(0) = w
\end{aligned}
\tag{4}
$$

Using the martingale approach[5], we can transform the differential equation of wealth dynamics into the form of expectations. After multiplying the derivative of discounted wealth process $d(e^{-rt}W)$ and taking Ito's integral, the budget constraint can be changed to the expected sum of the discounted consumption process by the local martingale property. In equilibrium, the agent invests all her wealth in the stock, so the control variable is changed into a terminal wealth.

Problem 2.2 *The agent maximizes a utility with a budget constraint*

$$
\begin{aligned}
&V(w) = \sup_{W_T} E\left[u(W_T)\right] \\
&s.t \\
&E^Q\left[e^{-rT}W_T\right] \le w \Leftrightarrow E\left[H_T W_T\right] \le w
\end{aligned}
\tag{5}
$$

2.2 Problem with model uncertainty

Based on the model uncertainty framework[6], we derive the investor's risk aversion function under model uncertainty. A robust agent, who lives in the model uncertainty world, has both a reference model and a worst-case alternative model. A worst-case alternative model is assumed to have a distorted drift of a reference wealth dynamics.

$$
\begin{aligned}
&dW_t = \mu(W_t)dt + \sigma(W_t)dB_t = \left\{rW_t + (\mu - r)\pi\right\}dt + \pi_t \sigma dB_t \\
&dW_t^a = \left[\mu(W_t) + \sigma(W_t)^2 h(W_t)\right]dt + \sigma(W_t)dB_t \\
&\textit{where,} \\
&\mu(W_t) = rW_t + (\mu - r)\pi_t, \ \sigma(W_t) = \pi_t \sigma, \ h(W_t) \ \textit{is arbitrary process}
\end{aligned}
\tag{6}
$$

[5] See Cox and Huang (1989) and Karatzas, Lehoczky and Shreve (1987)
[6] Anderson, Hansen, and Sargent (2003) and Hansen and Sargent (2001, 2008)

Given a maximization problem, a robust agent wants to minimize the relative entropy[7], which is measured as the distance between the reference model and the worst-case alternative model. Controlling the arbitrary function $h(W_t)$, a robust agent tries to minimize the relative entropy in the following min-max utility problem. The inverse of the coefficient of relative entropy $R(Q)$ represents an aversive attitude of pessimistic events. If the parameter ψ goes to infinity, the robust agent has more adverse distortions $h(W_t)$ in the drift of wealth dynamics. This implies that the agent do not believe reference wealth dynamics. In contrast, as the parameter ψ approaches to zero, the agent has zero distortions, which means that the agent never fears a worst case scenario. So, the case where $\psi=0$ is identical to problem 2.1.

Problem 2.3 *The robust agent faces a min-max problem with a budget constraint*

$$
\begin{aligned}
&V(w) = \inf_{h} \sup_{\pi_t} E\left[u(W_T)\right] + \frac{1}{\psi} R(Q) \\
&s.t \\
&dW_t^a = \left[\mu(W_t) + \sigma(W_t)^2 h(W_t)\right] dt + \sigma(W_t) dB_t \\
&where, \\
&R(Q) = \frac{1}{2} E\left[\sigma(W_T)^2 h(W_T)^2\right]
\end{aligned}
\tag{7}
$$

Similar to problem 2.2, we replace the differential form of wealth dynamics with the expected sum of the discounted consumption process. Since the portfolio weight equals the level of wealth in equilibrium, we set π_t. equal to W_T, which gives the following problem.

Problem 2.4 *The robust agent maximizes her utility with a budget constraint*

$$
\begin{aligned}
&V(w) = \inf_{h} \sup_{W_T} E\left[u(W_T)\right] + \frac{1}{2\psi} E\left[W_T^2 \sigma^2 h(W_T)^2\right] \\
&s.t \\
&E\left[H_T \cdot W_T\right] \le w + E\left[H_T \cdot W_T^2 \sigma^2 h(W_T)\right]
\end{aligned}
\tag{8}
$$

[7] Relative entropy $R(Q)$ is defined by the expectation of log likelihood of Randon-Nikodym derivative.

2.3 Solution

To obtain the optimal solution for problem 2.4, let us define the following Lagrangian function L, where is a Lagrangian multiplier.

$$L\left(h, W_T, \lambda\right) = u\left(W_T\right) + \frac{1}{2\psi} W_T^2 \sigma^2 h\left(W_T\right)^2 + \lambda\left(w + H_T \cdot W_T^2 \sigma^2 h\left(W_T\right) - H_T \cdot W_T\right)$$

$$\begin{aligned} &F.O.C\big|_h \Rightarrow h = -\lambda\psi H_T \\ &u'\left(W_T\right) = \lambda H_T + \lambda\xi H_T^2 \\ &\textit{where,} \\ &\xi = \lambda\psi W_T \sigma^2 \end{aligned} \tag{9}$$

The first order condition implies that the uncertainty aversion parameter ψ is negatively related to the distortion of drift h. This relationship gives two implications. First, as the uncertainty aversion parameter ψ increases, the agent faces more negatively distorted wealth dynamics with more fear. Second, when the stochastic discount factor is higher, the more negative distortions the agent has. In the bad economy, since the aversive attitude about pessimistic events and stochastic discount factor is higher in general, it seems reasonable that a robust agent is more likely to have negative returns.

Next, by substituting the distorted process h into the Lagrangian function and taking a first order derivative with respect to wealth W_T, we derive the marginal utility which is composed of linear stochastic discount factor and its quadratic term. If the model uncertainty parameter ψ goes to zero, the marginal utility is equal to the linear coefficient of the stochastic discount factor, which is a conventional form without model uncertainty. As the uncertainty parameter increases, that is as the agent more fears the pessimistic scenario, the marginal utility increases. Especially additional increase of marginal utility is affected by the quadratic term of both the level of pricing kernel H_T and the volatility of stock price σ.

With second derivative over first derivative with respect to wealth in the equation (9), we derive the investor's absolute risk aversion (ARA) by eliminating the shadow price λ. Since the stochastic discount factor is calculated as the ratio of the risk-neutral probability *Q(W)* to the subjective probability *P(W)*, we finally derive the main proposition about the option-implied absolute risk aversion under model uncertainty.

Proposition 2.1 *The absolute risk aversion (ARA) under model uncertainty is*

$$\begin{aligned} ARA_{unc} &= -\frac{u''(W_T)}{u'(W_T)} = -\frac{H_T'}{H_T} - \frac{\xi H_T'}{1+\xi H_T} \\ &= \left(\frac{P'(W)}{P(W)} - \frac{Q'(W)}{Q(W)} \right) \left(\frac{P(W)+2\xi Q(W)}{P(W)+\xi Q(W)} \right) \\ &= ARA_0 \left(1 + \frac{\xi Q(W)}{P(W)+\xi Q(W)} \right) \end{aligned} \tag{10}$$

The first implication of proposition 2.1 is that absolute risk aversion with model uncertainty (ARA_{unc}) is higher than that with model uncertainty (ARA_0). As the model uncertainty parameter ψ increases, ARA_{unc} also increases. In particular, when the parameter ψ is equal to zero, the absolute risk aversion is identical to the case of Jackwerth (2000) and Ait-Sahalia (2000). If the parameter ψ approaches to infinite, ARA_{unc} converges two times of ARA_0. Likewise, a model uncertainty about the pessimistic scenario could bring about more risk aversive preferences than the case with only a reference model.

The second implication is that the absolute risk aversion induced by option-implied uncertainty is counter-cyclical. Since the increments in absolute risk aversion is proportional to the quadratic level of pricing kernel, the increments of absolute risk aversion enlarges when the economy is bad. On the contrary, when the economy is good, the pricing kernel decreases. So, the level of absolute risk aversion in good state is less than the absolute risk aversion in bad state. This decreasing option-implied uncertainty premium across wealth can be applied to account for the smirk pattern of option-

implied volatility. Since the model uncertainty parameter ψ interacts with the power term of the stochastic discount factor, the robust agent has a highly skewed absolute risk aversion function in the negative wealth region.

To investigate the shape of option implied risk aversion functions with model uncertainty, we require the estimated pricing kernel and the model uncertainty parameter. We assume that the pricing kernel is the following Chebyshev polynomial function suggested in Rosenberg and Engle (2002). They state that the Chebyshev polynomial specification more effectively estimates empirical pricing kernels than the power specification. Figure 1 shows that the pricing kernel with is negatively sloped across wealth. As the wealth decreases, the pricing kernel becomes more negatively skewed.

$$\begin{aligned} &h(W) = \theta_0 T_0 \exp\left(\theta_1 T_1(W) + \theta_2 T_2(W) + \theta_3 T_3(W)\right), where \\ &T_n(x) = \cos\left(n \cdot \cos^{-1}(x)\right), \theta_0 = 0.1, \theta_1 = -2, \theta_2 = -1, \theta_3 = -1 \end{aligned} \tag{11}$$

[Figure 1 about here]

Based on the estimated pricing kernel, we numerically derive the option-implied risk aversion functions of proposition 2.1 when the model uncertainty parameter ψ is 0, 1, 5, and 100. Figure 2 demonstrates that the absolute risk aversion functions decrease across wealth, where the model uncertainty parameter ψ plays a role in making the functional shape steep. As the model uncertainty parameter increases, which implies that the agent more faces pessimistic scenario, the marginal value of option-implied risk aversion functions becomes higher.

[Figure 2 about here]

2.4 Option-Implied Uncertainty Aversion

Next, we suggest a method to estimate a reasonable level of model uncertainty premium separated from a general equity premium by using the detection-error probabilities developed by Anderson, Hansen, and Sargent (2003) and Hansen and Sargent (2008). The detection-error probability is defined as the equally weighted sum of two mistake probabilities p_A and p_B, where p_A is the probability of mistakenly choosing the worst-case model when the reference model holds, and the p_B is the probability of mistakenly choosing the reference model when the worst-case alternative model holds.

$$p_\varepsilon = \frac{1}{2}\Pr\left(\zeta < 0 \middle| A\right) + \frac{1}{2}\Pr\left(\zeta > 0 \middle| B\right) \qquad (12)$$
$$where, \zeta = \log\ likelihood\ ratio$$

When the reference model and the worst-case alternative model both follow a geometric Brownian motion, the detection error probability can be calculated by the difference of the equity premium of the two models[8]. We define the model uncertainty premium as the difference between the equity premium without model uncertainty and the pessimistic equity premium of the robust investor. In equilibrium, since the optimal investment in risky assets is equal to the total remaining wealth, the robust agent's equity premium (=EP_{unc}) is $ARA_{unc}\cdot\sigma^2$ and the equity premium without model uncertainty (=EP_0) is $ARA\cdot\sigma^2$ under the assumption of CRRA utility. The model uncertainty premium measured by the distance between two models is affected by model uncertainty parameter ψ as well as a traditional absolute risk aversion.

By substituting the absolute risk aversion for density functions *P(W), Q(W)* of proposition 2.1, we derive the following option-implied detection-error probability, which is affected by the model uncertainty parameter ψ, the subjective density *P(W)*, and the risk-neutral density *Q(W)*. The detection-error probability is getting lower when the model uncertainty parameter ψ increases. This

[8] See Maenhout (2004)

implies that as the robust agent more worries about the worst-case pessimistic scenario, she easily distinguishes which model holds between reference model and the alternative worst-case model.

$$
\begin{aligned}
p_{\varepsilon} &= \Pr\left[x < -\left(\frac{EP_{unc} - EP_0}{2\sigma} \right) \sqrt{N} \right] \\
&= \Pr\left[x < -\frac{1}{2\sigma} \left(\frac{P'(W)}{P(W)} - \frac{Q'(W)}{Q(W)} \right) \left(\frac{\xi Q(W)}{P(W) + \xi Q(W)} \right) \sqrt{N} \right] \qquad (13) \\
&\textit{where, } N = \textit{number of sample}
\end{aligned}
$$

Figure 3 plots the model uncertainty premium when the pricing kernel takes the form of equation (11) and the model uncertainty parameter ψ is 1, 5, and 100. As stated in the equation (13), the model uncertainty premium increases as the model uncertainty parameter ψ is higher. When the parameter ψ is 100 at 85% wealth level, the model uncertainty premium is about 18% that is as twice as the case of ψ=1. Interestingly, the model uncertainty premium enlarges as the level of wealth decreases. This decreasing property of option-implied uncertainty premium looks similar to the smirk pattern of option-implied volatility. The higher implied volatility at lower strike prices could be attributed to require higher uncertainty premium at negative wealth regions.

[Figure 3 about here]

3. Empirical Analysis

With traded option database, we suggest both empirical option-implied risk aversion functions and plausible empirical option-implied uncertainty premium based on the proposition 2.1 and equation (13). As shown in proposition 2.1, the robust agent's absolute risk aversion is determined by subjective probability, risk-neutral probability, and the model uncertainty parameter. After estimating

subjective probability and risk-neutral probability, we extract the empirical option-implied risk aversion functions and the empirical option-implied uncertainty premium.

We use S&P 500 index options from the OptionMetrics Ivy Database from July 1, 1996 through September 30, 2008. The OptionMetrics Ivy Database has the best bid and ask price of closing day across different strike prices. We calculate the mid-price between bid and ask price, and we choose options series with maturities closest to one month. We do not include options that are not traded daily or deep OTM options with an absolute value of delta of less than 0.01. Also, we eliminate data that violate the option arbitrage conditions[9]. As an underlying asset, we calculate a daily future-based index return from the S&P 500 index in the OptionMetrics Ivy Database. For the interest rates, we use three-month Euro-dollar LIBOR rates in the OptionMetrics Ivy Database.

For estimating subjective density, we use the following GJR-GARCH (1,1) model which is developed in Glosten et al. (1993). The GJR-GARCH model is characterized by capturing that the second moment is negative correlated with an underlying return. First, we estimate GJR-GARCH (1,1) parameters of table 1 by maximizing the log likelihood of S&P 500 returns. Next, we calculate the one month subjective density of S&P 500 index after 200,000 times' monte-carlo simulations of estimated GJR-GARCH (1,1) with a four-year standardized innovation(ε_t/σ_t) every month. By applying a Gaussian kernel density[10] to the continuous function, we finally obtain the average of the estimated subjective density.

$$\begin{aligned} &\ln\left(S_t / S_{t-1}\right) - r_f = \mu + \varepsilon_t,\ \varepsilon_t \sim N\left(0, \sigma_t^2\right) \\ &\sigma_t^2 = \alpha_0 + \alpha_1 \varepsilon_{t-1}^2 + \beta \sigma_{t-1}^2 + \delta \max\left[0, -\varepsilon_{t-1}\right]^2 \ : \text{GJR-GARCH}\ (1,\ 1) \\ &\sigma_t^2 = \alpha_0 + \alpha_1 \varepsilon_{t-1}^2 + \beta \sigma_{t-1}^2 \qquad\qquad\qquad\quad : \text{GARCH}\ (1,\ 1) \end{aligned} \tag{14}$$

[9] $C(K,T) \geq S - e^{-rT}K - D_T, P(K,T) \geq e^{-rT}K - S + D_T$, where C is call option's price, P is put option's price, K is strike Price, T is yearly based time to maturity, S is underlying asset, r is risk-free rate, and D_T is sum of discounted daily dividend during time T.

[10] The bandwidth is equal to $\frac{1.8\sigma}{\sqrt[5]{N}}$, where σ is the standard deviation of returns, and N is the number of observations.

[Table 1 about here]

Figure 4 shows the average of estimated subjective densities compared to the average of historical one month densities from July, 1996 through September, 2008. The GJR-GARCH(1,1) based subjective density is more concentrated around the average return and negatively skewed than the actual historical density.

[Figure 4 about here]

Next, we extract risk-neutral densities with a formula of Breeden and Litzenberger (1978), which states that the discounted risk-neutral density is equal to the second derivative of call option prices with respect to the option strike prices K as follows.

$$e^{-rT} q(K) = \frac{\partial^2 C(K)}{\partial K^2} \tag{15}$$

We use a Shimko (1993)'s method of smoothing implied volatility in the framework of non-parametric approach. Shimko (1993) suggests an estimation methodology of implied volatility surface with respect to the strike price by assuming that the implied volatility is a quadratic function of strike price. Similarly, applying ordinary least squares, we estimate implied volatility surfaces of observed call options with one month maturity every month from July, 1996 through September, 2008. The following graph shows the average of estimated implied volatility for every month, which looks similar to the smirk pattern stated in Rubinstein (1994).

[Figure 5 about here]

After substituting estimated implied volatility into the Black-Sholes formula, we derive the approximated risk-neutral density based on the equation (14). The L.H.S's risk-neutral density can be simply obtained by applying the finite difference method of R.H.S. The following graph shows the option-implied risk-neutral density compared to the estimated subjective density with GJR-GARCH (1, 1). The more convex an implied volatility surface across strike prices, the higher fat tail an implied risk-neutral density has. Negatively sloped implied volatility surface brings about negative skewness in risk-neutral density. As known in Girsanov theorem, the risk-neutral density is negatively distorted by risk premiums compared to the subjective density.

[Figure 6 about here]

With empirically estimated subjective density and risk-neutral density, we extract an empirical option-implied risk aversion function that is derived in proposition 2.1. Figure 7 illustrates that the option-implied risk aversion function decreases across wealth in general and slightly increases in the positive region of wealth. As the model uncertainty parameter increases, the option-implied risk aversion becomes steeper. Especially, in the negative wealth region, the uncertainty aversive preference about a pessimistic scenario has a greater influence on the risk aversion functions. The more a robust agent considers the worst-case scenario, the higher level of option-implied risk aversion. But the increment of option-implied risk aversion induced by model uncertainty is limited by two times of traditional option-implied risk aversion without model uncertainty.

[Figure 7 about here]

Besides the assumption of model uncertainty parameter ξ, if we know the reasonable value[11] of detection-error probability for the difference between the reference model and the alternative model, it

[11] Hansen and Sargent (2008) recommend the 10% level of detection-error probability as a reasonable value to distinguish the reference model and the alternative model.

is plausible to estimate the model uncertainty parameter ξ. Hansen and Sargent (2008) recommend the 10% level of detection-error probability as a reasonable value to distinguish two models. In the range of wealth level between 0.9 and 1.1, we attempt to choose the parameter by minimizing the following mean-square error of the detection-error probability stated in equation (12).

$$p_{\varepsilon}(W) = \min_{\xi} \sum_{W=0.9}^{1.1} \left(\Pr\left[x < -\frac{1}{2\sigma} \left(\frac{P'(W)}{P(W)} - \frac{Q'(W)}{Q(W)} \right) \left(\frac{\xi Q(W)}{P(W) + \xi Q(W)} \right) \sqrt{N} \right] - P_d \right)^2 \qquad (16)$$

$$where, P_d \in \{0.1, 0.2, 0.3\}$$

Table 2 reports that the model uncertainty parameter ξ is estimated 2.06 with 10% detection-error probability. As the detection-error probability increases, the estimated model uncertainty parameter decreases. For example, considering 20% detection-error probability, the model uncertainty parameter ξ becomes 1.24. This implies that it is easier for the robust agent to distinguish the reference model and the worst case alternative model when the model uncertainty preference increases.

With empirically estimated model uncertainty parameter ξ, we plot the empirical option-implied uncertainty premium (=EP_{unc} - EP_0). Figure 8 illustrates that the empirical option-implied uncertainty premium shows steeper pattern across wealth especially negative return of wealth. Our empirical option-implied uncertainty premium looks very similar to the shape of volatility spread, which is defined by the difference between the implied volatility and historical volatility. This phenomenon of negative volatility spread could be explained by the option-implied uncertainty premium regarding the aversive attitude about a pessimistic scenario.

[Figure 8 about here]

4. Conclusion

We construct a simple equilibrium model for deriving option-implied preferences with model uncertainty that is differentiated from the aversive attitude about tail risk of known distribution. Our theoretical model shows that a robust agent with model uncertainty has higher absolute risk aversion than an agent without model uncertainty. As the robust agent fears more pessimistic scenario, the agent's option-implied risk aversion function is getting higher. The level of option-implied risk aversion with model uncertainty can be twice as much as that without model uncertainty.

With empirically estimated subjective density and risk-neutral density of S&P 500 index, we suggest empirically estimated option-implied risk aversion functions and related option-implied uncertainty premium. Empirical analysis shows that higher level of model uncertainty, a larger option-implied risk aversion and a steeper shape are derived. Also, empirically estimated option-implied uncertainty premium shows a steeper smirk pattern of negative wealth regions, which is helpful for explaining the smirk pattern of option-implied volatility surface and negative volatility spread between an implied volatility and a historical volatility.

BIBLIOGRAPHY

Aït-Sahalia, Y., & Lo, A. (2000). Nonparametric risk management and implied risk aversion. Journal of Econometrics, 94, 9-51.

Anderson, E., Hansen, L., & Sargent, T. (2003). A quartet of semigroups for model specification, robustness, prices of risk, and model detection. Journal of European Economic Association, 1, 68-123.

Bakshi, G., & Kapadia, N. (2003). Delta-hedged gains and the negative market volatility risk premium. Review of Financial Studies, 16, 527-266.

Bakshi, G., & Madan, D. (2006). A theory of volatility spreads. Management Science, 52, 1945-1956.

Bliss, R. R., & Panigirtzoglou, N. (2004). Option implied risk aversion estimate. Journal of Finance, 59, 407-446.

Breeden, D. T., & Litzenberger, R.H. (1978). Prices of state-contingent claims implicit in option prices. Journal of Business, 51, 621-651.

Chen, Z., & Epstein, L. (2002). Ambiguity, risk and asset returns in continuous time. Econometrica, 70, 1403-1443.

Cox, J.C., & Huang C. F. (1989). Optimal consumption and portfolio policies when asset prices follow a diffusion process. Journal of Economic Theory, 39, 33-83.

Ellsberg, D. (1961). Risk, ambiguity, and the savage axioms. Quarterly Journal of Economics, 75, 643-669.

Epstein, L., & Wang, T. (1994). Intertemporal asset pricing under knightian uncertainty. Econometrica, 62, 283-322.

Gilboa, I., & Schmeidler, D. (1989). (1989). Max-min expected utility with non-unique prior. Journal of Mathematical Economics, 18, 141-153.

Glosten, L.R., Jagannathan, R., & Runkle, D.E. (1993). On the relation between the expected value and the volatility of the nominal excess return on stocks. Journal of Finance, 48, 1779-1801.

Hansen, L, & Sargent T. (2001). Robust control and model uncertainty. American Economic Review, 91, 60-66.

Hansen, L, & Sargent T. (2008). Robustness. Princeton University Press, 2008.

Kang, B. J., & Kim, T. S. (2006). Option-implied risk preferences: an extension to wider classes of utility functions. Journal of Financial Markets, 9, 180-198.

Karatzas, I., Lehoczky J., & Shreve, S. E. (1987). Optimal portfolio and consumption decisions for a small investor on a finite horizon. SIAM Journal of Control and Optimization, 25, 1557-1586.

Knight, F. (1921). Risk, uncertainty and profit. Boston: Houghton Mifflin.

Jackwerth, J. C. (200). Recovering risk aversion from option prices and realized returns. Review of Financial Studies, 13, 433-451.

Lien, D., & Wang, Y. (2003). Futures market equilibrium under knightian uncertainty. Journal of Futures Market, 7, 701-718.

Liu, J., Pan, T., & Wang, T. (2005). An equilibrium model of rare-event premia and its implication for option smirks. Review of Financial Studies, 18, 131-164.

Maenhout, P. (2004). Robust portfolio rules and asset pricing Review of Financial Studies, 17, 951-983.

Maenhout, P. (2006). Robust portfolio rules and detection error probabilities for a mean-reverting risk premium. Journal of Economic Theory, 128, 136-163.

Rosenberg, J. V., & Engle, R. F. (2002). Empirical pricing kernels. Journal of Financial Economics, 64, 341-372.

Rubinstein, M., (1994). Implied binomial trees. Journal of Finance, 49, 771-818.

Shimko, D. (1993). Bounds of probability. Risk, 6, 34-37.

Ziegler, A., (2007). Why does implied risk aversion smile? Review of Financial Studies, 20, 859-904.

Figure 1. Pricing kernel with Chebyshev polynomial function

Figure 1 graphs the empirical pricing kernel when it takes a form of Chebyshev polynomial function of equation (11). This empirical pricing kernel decreases across the level of wealth, and the slope is steeper for negative regions of wealth than the positive regions of wealth. It ranges between 0.96 and 1.05 for the wealth level of [0.85, 1.1].

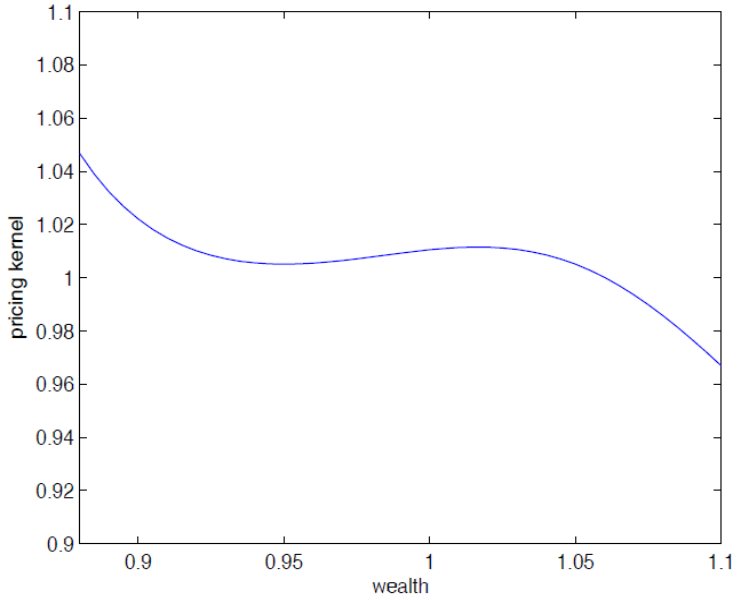

Figure 2. Empirical option-implied risk aversion function with Chebyshev polynomial function

Figure 2 shows the option-implied risk aversion functions with model uncertainty derived in the proposition 2.1. Assuming the pricing kernel follows a Chebyshev polynomial function of equation (11), we estimate the option-implied risk aversion functions when the model uncertainty parameter ξ is 0, 1, 5, and 100. As the wealth level increases, the level of option-implied risk aversion is higher in the range of [0, 10]. When the model uncertainty parameter is higher, the option-implied risk aversion with model uncertainty also increases. The increment induced by model uncertainty is limited as twice as the option-implied risk aversion without model uncertainty.

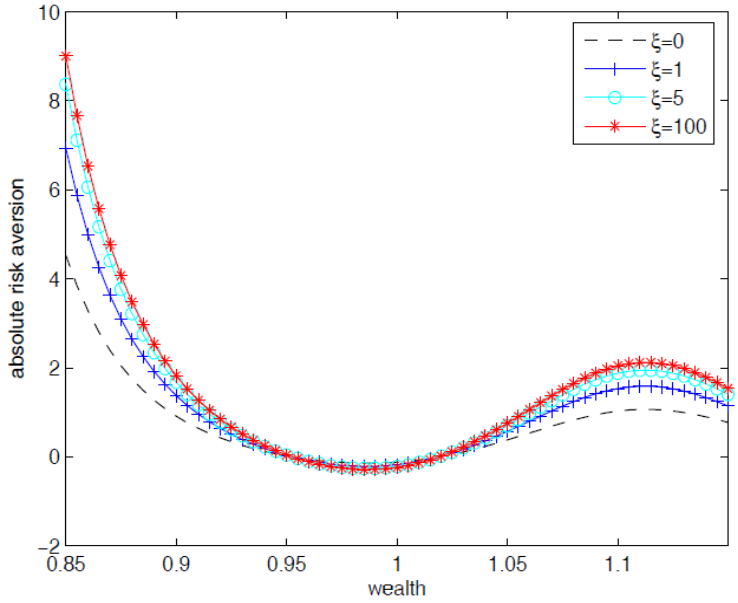

Figure 3. Option-implied uncertainty premium with Chebyshev polynomial function

Figure 3 graphs the option-implied uncertainty premium which is defined by the difference between an equity premium with model uncertainty and an equity premium without model uncertainty. When the pricing kernel follows a Chebyshev polynomial function of equation (11), we numerically calculate option-implied uncertainty premium. This model uncertainty premium decreases and shows a smirk pattern across wealth. As the model uncertainty parameter ξ increases, both the level of model uncertainty premium and the negative slope are getting higher. The average value of the option-implied uncertainty premium is 4.27%, 6.73%, and 12.39% respectively when ξ is 1, 5, and 100.

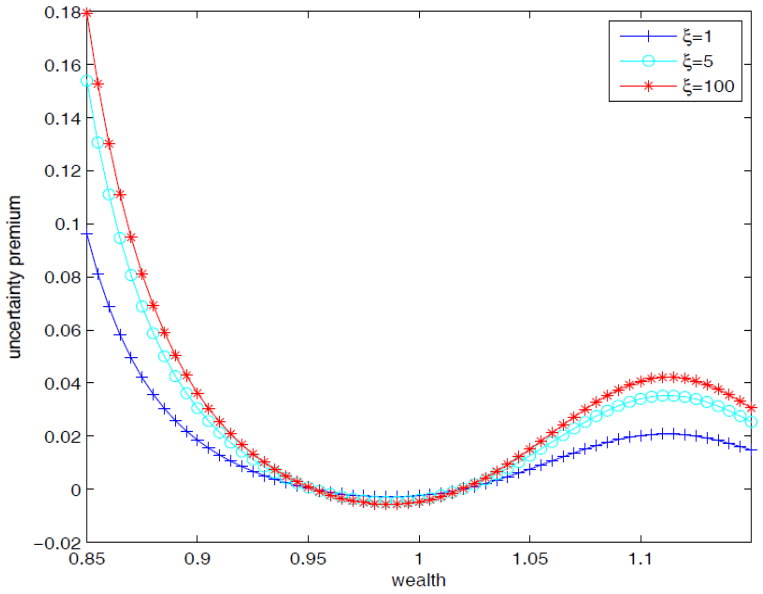

Figure 4. Empirical subjective density

Figure 4 graphs the subjective density based on the GJR-GARCH (1, 1) model, which is expressed in a bold line. After estimating GJR-GARCH (1, 1) parameters of equation (14), we estimate subjective densities of S&P 500 index returns with 200,000 Monte Carlo simulations over four year empirical innovation density. Then we apply a Gaussian kernel with bandwidth $\frac{1.8\sigma}{\sqrt[5]{N}}$ and use the average of estimated subjective densities. For comparison, we give a dotted line of the average of simple historical densities. The GJR-GARCH (1, 1) based subjective density is slightly negative distorted than the historical density.

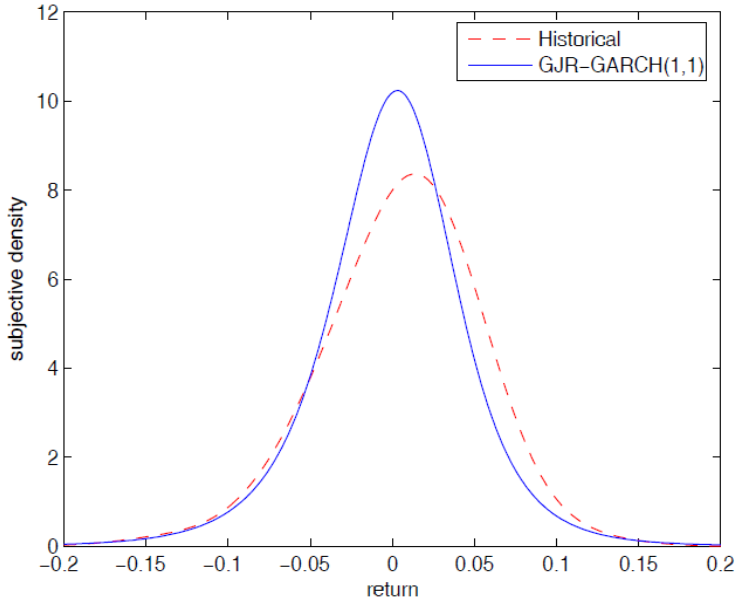

Figure 5. Implied volatility of S&P 500 index options

Figure 5 shows the smirk pattern of implied volatility of S&P 500 index options across option moneyness (=strike/spot). We use S&P 500 index options of OptionMetrics Ivy Database from July 1996, through September, 2008. Assuming that the implied volatility is a quadratic function of strike prices such that $\sigma = a_0 + a_1 K + a_2 K^2$, we estimate a_0, a_1, a_2 every month. All samples show statistically in the 95% confidence level. Then we average monthly estimated implied volatility of S&P index options, which ranges between 0.17 and 0.29.

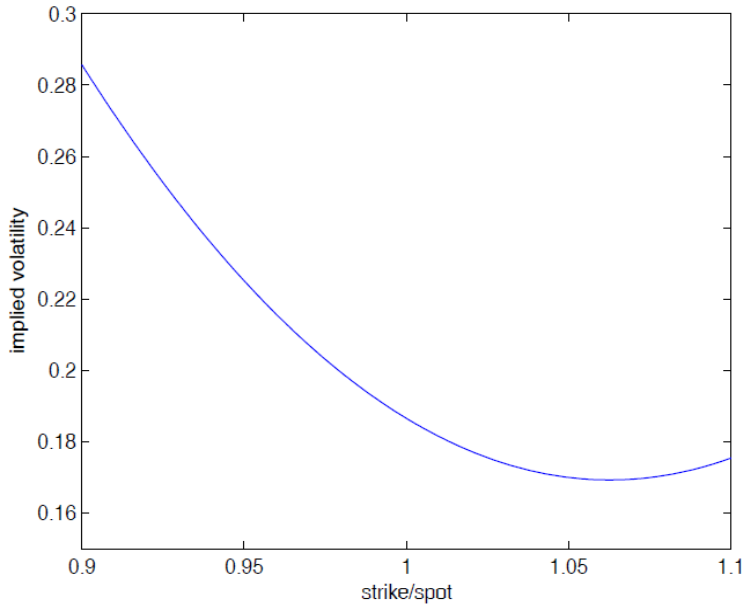

Figure 6. Empirical risk-neutral density

Figure 6 graphs the risk-neutral density extracted from S&P 500 index options. Based on the equation (15), we approximate the risk-neutral density with finite difference method such that $q(K) = e^{rT}[\frac{C(K+\Delta K)-2C(K)+C(K-\Delta K)}{(\Delta K)^2}]$. We estimate risk-neutral densities every month and average risk-neutral densities from July, 1996 through September, 2008. Compared to the GJR-GARCH (1, 1) based subjective density, the risk-neutral density is little left-skewed.

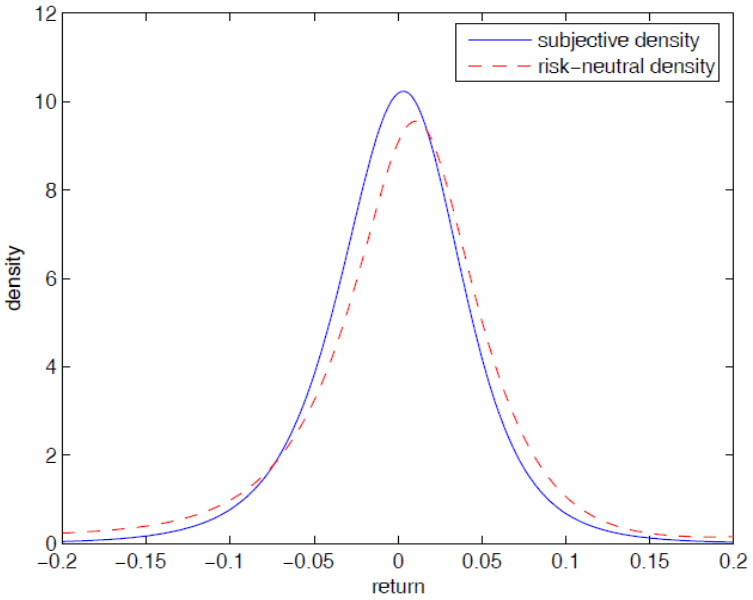

Figure 7. Empirical option-implied risk aversion functions with model uncertainty

Figure 7 graphs the empirical option-implied risk aversion functions with estimated subjective density and risk-neutral density. Similar to the numerical shape of Figure 2, the empirical option-implied risk aversion decreases across wealth in general and slightly increases in the positive wealth regions, which ranges -10 and 25. As the model uncertainty parameter increases, the empirical option-implied risk aversion and the slope becomes higher.

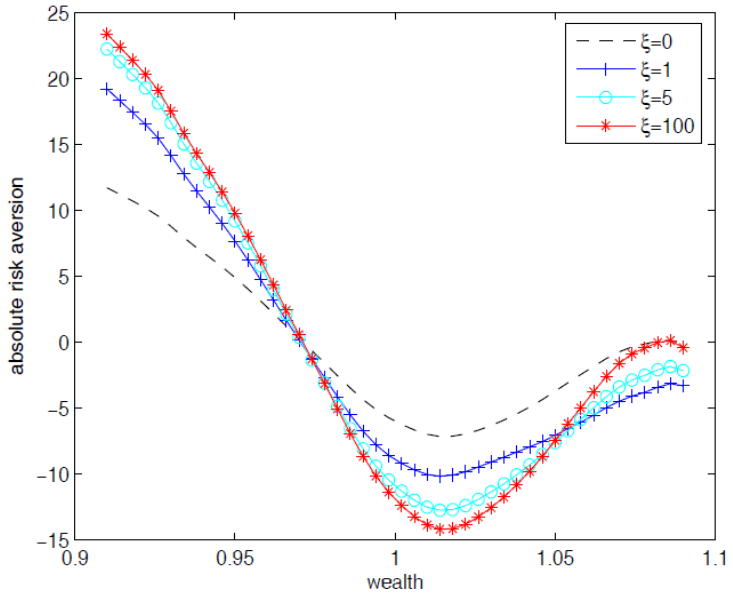

Figure 8. Empirical option-implied uncertainty premium

Figure 8 graphs the empirical option-implied uncertainty premium when the detection-error probabilities are 10%, 20%, and 30% respectively. The lower-detection error probability, which implies that the agent more fears about a pessimistic scenario, the empirical option-implied uncertainty premium becomes steeper. At 0.9's wealth level, estimated uncertainty premium are 2%, 4%, and 6% when the detection-error probabilities are 10%, 20%, and 30% respectively.

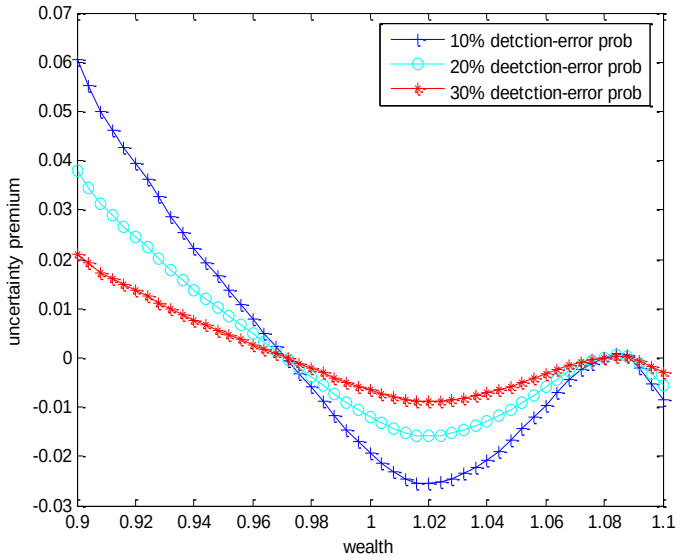

Table 1. GJR-GARCH (1, 1) and GARCH (1, 1) estimation

Table 1 reports the estimation result of GJR-GARCH (1, 1) and GARCH (1, 1) model stated in equation (14). We use daily based S&P 500 index returns from Jan 1, 1970 to Sep 30, 2008. All coefficients are statistically significant, and the log-likelihood of GJR-GARCH (1, 1) is higher than that of GARCH (1, 1). To extract subjective density, we use GJR-GARCH (1, 1) model instead of GARCH (1, 1) model.

GJR-GARCH (1, 1)

parameter	coefficient	standard errors	t-statistics
α_0	1.0991E-06	8.0180E-05	3.31
α_1	0.0205	0.0034	6.10
β	0.9277	0.0027	339.24
δ	0.0827	0.0039	21.07
Log-likelihood	32523.09		

GARCH (1, 1)

parameter	coefficient	standard errors	t-statistics
α_0	1.0991E-06	8.0180E-05	3.31
α_1	0.0205	0.0034	6.10
β	0.9277	0.0027	339.24
Log-likelihood	32523.09		

Table 2. Estimation of option-implied model uncertainty parameter

Table 2 reports the estimation result of option-implied uncertainty parameter ξ based on equation (16). As input variables of equation (16), we use the average of subjective density from GJR-GARCH (1, 1) and the average of risk-neutral density from equation (15). For the underlying asset's volatility, we use annualized historical volatility σ = 0.2086 during sample periods. Estimation results show that the model uncertainty parameter which represents for the aversive attitude about the worst-case scenario increases as the detection-error probability decreases.

Option-implied model uncertainty parameter

Detection-error probability	ξ
10%	2.0619
20%	1.2390
30%	0.6676